Multi-Channel MFSK Modulation and Demodulation through Short-Range, Large-Bandwidth, Underwater Acoustic Channels

William F. Jenkins II[1], Joseph A. Rice[2], Lawrence J. Ziomek[2], Dale Green[3]

[1]United States Navy, **wjenkins@nps.edu**

[2]Naval Postgraduate School, 1 University Circle, Monterey, California 93940, United States, {**rice,ziomek**}**@nps.edu**

[3]Teledyne Benthos Inc., 49 Edgerton Drive, North Falmouth, Massachusetts 02556, United States, **dgreen2@teledyne.com**

We propose a scheme for short-range (<500 m) communications in shallow water which is a variation on an existing commercial acoustic modem reliably used for medium-range (<5 km) communications in the 9-14 kHz band. The proposed scheme exploits higher acoustic frequencies and increased spectral bandwidth compatible with the short-range link, thus increasing the channel capacity. The existing commercial modem combines principles of M-ary frequency-shift keying (MFSK) and orthogonal frequency-division multiplexing (OFDM) in a method commonly referred to as multi-channel MFSK. We provide analytical expressions for the existing modulation in the form of 32 orthogonally spaced channels, each containing a 4-ary FSK pulse train. We expand the original modulation band of 5 kHz using either bandwidth scaling or multiplexing, and implement various candidate modulations with bandwidths of 10 and 20 kHz. Of concern for short-range links in shallow water is multipath propagation with large time-spread and the possibility of significant intersymbol interference (ISI). For various shallow-water test environments, we perform physics-based propagation modeling, estimate the impulse response, determine the dominant eigenray paths, and calculate channel time-spread. We evaluate the candidate modulations in these test environments and assess their immunity against ISI.

1 Introduction

The United States Navy's development of Seastar, an underwater acoustic local area network (LAN) concept [1, 2], has motivated an investigation into how intersymbol interference (ISI) affects short-range, high-frequency communications. The modulation scheme used for Seastar is a variation of the one employed by the Seaweb underwater acoustic wide area network (WAN). The modulation scheme combines principles of traditional M-ary frequency-shift keying (MFSK) and frequency-division multiplexing (FDM) to form a scheme referred to as multi-channel MFSK.

The scope of this paper includes a mathematical description of the multi-channel MFSK modulation scheme. Various candidate implementations of the scheme are subsequently evaluated for their immunity against ISI in a variety of shallow-water geometries.

2 The Underwater Acoustic Communication Channel

In the general context of underwater acoustic communication, we may treat the ocean as a wideband, frequency-dependent, linear, time- and space-variant filter [3]. As we seek to evaluate ISI, we are specifically concerned with a multipath-induced fading channel, in which multiple versions of the transmitted signal arrive at a receiver. Based on the physical characteristics of the channel, each of the multipath arrivals exhibits a unique amplitude decay, time delay, phase shift and frequency shift dependent on the path's unique propagation. This propagation is highly frequency-dependent, and in underwater acoustic communication, has been described with the use of the acoustic link budget [4, 5, 6]:

$$\mathrm{SNR}_a\ (\mathrm{dB}) = \mathrm{SL} + \mathrm{DI} - (\mathrm{TL} + \mathrm{NL}) \tag{1}$$

where SNR_a is the acoustic signal-to-noise power ratio (in dB), SL is the source level (in dB re 1 μPa @ 1 m), DI is the directivity index (in dB), TL is the transmission loss (in dB), and NL is the ambient noise level (in dB re 1 $\mu\mathrm{Pa}^2$).

Physics-based propagation modeling was accomplished using the Bellhop acoustic ray tracing program, which identifies eigenrays and determines their times of arrival, phase shifts due to boundary interactions, and amplitudes [7]. The version of Bellhop used for this research was coupled to a bottom-loss model called Bounce [7].

In order to more clearly illustrate the time/frequency relationships for the various candidate modulation schemes, simulations were conducted in a more simplified environment than what would be found in a natural environment. We subsequently define the shallow, short-range underwater communication channel to consist of a homogeneous body of seawater with a constant sound-speed profile of 1500 m/s and density of 1026 kg/m^3 [8], extending from the surface to a bottom half-space located at a depth of 205 m, and ranging from 0 to 500 m. The bottom half-space was assumed to be a fluid-like sea bottom consisting of quartz sand, with a sound speed of 1730 m/s and a density of 2070 kg/m^3 [8]. Zero root-mean-square roughness was assumed for both the surface and bottom boundaries.

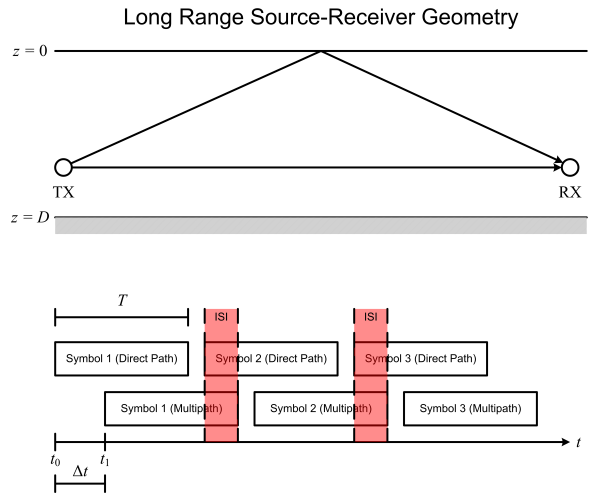

Figure 1: Direct path and surface-reflected path pulse trains for a long-range source-receiver geometry.

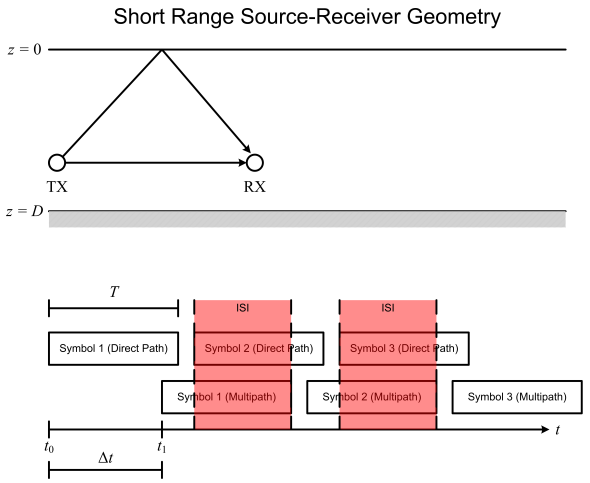

Figure 2: Direct path and surface-reflected path pulse trains for a short-range source-receiver geometry.

2.1 Intersymbol Interference

Intersymbol interference (ISI) occurs as a result of multipath propagation, when multiple received versions of the transmitted signal can result in constructive and destructive interference. Additional interference, known as interchannel interference (ICI), can occur when different frequencies are received simultaneously [9]. Both types of interference can lead to errors during demodulation, though ICI is minimized with the use of orthogonal signaling.

The effects of ISI become more pronounced in short-range, high-frequency communications. Figure (1) shows a long-range source-receiver configuration. Shown are two rays, a direct path and a surface-reflected path. The time difference of arrival between the two rays are depicted pictorially as pulse trains, and we see that, compared to the pulse duration T, this time difference is relatively small, corresponding to relatively small overlap between pulses, and therefore a lower degree of ISI. In Figure (2), a short-range source-receiver configuration is shown. In this case, the time difference of arrival is large compared to the pulse duration T, corresponding to relatively large overlap between pulses, and therefore a greater degree of ISI. Furthermore, if T is shortened, the overlap becomes even greater.

Another common way to describe the degree of multipath propagation is the channel time-spread, or multipath-spread, T_m, which is defined as the time over which the multipath signals arrive at the receiver [9]. Larger time-spread will coincide with larger time differences of arrival, and will increase the degree of ISI.

We can express the overlap shown in Figures (1) and (2) in terms of a ratio between the time difference of arrival between the direct path and the next multipath arrivals and the pulse duration T. This normalized time difference of arrival is, in a sense, a measure of the distance in time between two received pulses. We consider only the first multipath arrival for this comparison, as its amplitude is the greatest of all the multipath arrivals. The normalized time difference of arrival is given by:

$$\Delta t_N = \frac{t_1 - t_0}{T} \tag{2}$$

where t_0 and t_1 are the arrival times, in seconds, of the direct path and the next multipath arrivals, respectively, and T is the pulse duration in seconds. Thus, Eq.(2) describes how many symbols away in time the next multipath arrival is from the direct path arrival. For $\Delta t_N < 1$, the direct path pulse and the next multipath pulse overlap, and for $\Delta t_N > 1$, the next multipath pulse is interfering with a subsequent pulse other than the first. As an example, in the case where $\Delta t_N = 1$, the next multipath pulse begins just as the direct path pulse ends, and is consequently interfering with the second direct path pulse. Greater values for Δt_N thus correspond to an increased potential severity of ISI. It is important to emphasize that Δt_N is useful in evaluating *potential* ISI, since its value does not take into account phase shifts; in essence, it is a metric of a worst-case scenario.

3 Multi-Channel M-ary Frequency-Shift Keying

Both Seastar and Seaweb modems use a modulation scheme commonly referred to as multi-channel MFSK. However, this title is not entirely descriptive of how the modulation scheme actually works [2, 10]. We now present a mathematical representation of the multi-channel MFSK modulation scheme.

3.1 Modulation

Before representing multi-channel MFSK mathematically, it is useful and necessary to define pure MFSK. In MFSK

[11, 12, 13], M frequencies, each offset from a center frequency, are used to transmit M unique channel symbols; each symbol therefore corresponds to its own unique frequency.

Traditionally, the total number of channel symbols, and therefore frequencies, is determined by how many bits per symbol are used. However, in Seastar, due to signaling techniques applied before modulation, such as convolutional coding and interleaving, it is more accurate to replace our use of the word "bits" with "encoded symbols." This releases us from confusing bits that are truly fed into the communication system before coding and interleaving with bits that form channel symbols within the modulator. The number of possible channel symbols, and therefore frequencies, is thus determined by how many encoded symbols are used for each channel symbol.

In Seastar, there are two encoded symbols per channel symbol used. The number of unique channel symbols M is given by $M = 2^{n_b}$, where n_b is the number of encoded symbols per channel symbol. Seastar uses an M = 4 alphabet, so that there are four unique channel symbols, transmitted with four unique frequencies. This configuration is referred to as 1-in-4 FSK, or 4-ary FSK, because only one of a possible four unique transmission frequencies is actively transmitting at any instant [2, 10]. In the time domain, the MFSK waveform may be represented as a pulse train, and is given by [5]:

$$x(t) = \sum_{n=1}^{N} x_n(t - t_n), 0 \leq t \leq T_d \tag{3}$$

where the nth pulse, corresponding to one of the M symbols, is:

$$x_n(t) = A\cos(2\pi\left[f_c + \Delta f_n\right]t + \epsilon_n)\text{rect}\Big(\frac{t - 0.5T}{T}\Big) \tag{4}$$

where N is the number of pulses (channel symbols) transmitted in the time interval $0 \leq t \leq T_d$, t_n is the time instant when the nth pulse begins (seconds), T_d is the duration of the transmitted pulse train (seconds), A is the amplitude, f_c is the carrier frequency (hertz), Δf_n is the frequency offset of the nth pulse (hertz), ϵ_n is the introduced phase shift of the nth pulse (radians), T is the pulse or symbol duration (seconds), and

$$\text{rect}\Big(\frac{t - 0.5T}{T}\Big) = \begin{cases} 1, & 0 \leq t \leq T \\ 0, & \text{otherwise} \end{cases} \tag{5}$$

The total signal duration T_d can subsequently be expressed as NT seconds. The phase shift ϵ_n is included in Eq.(4) and subsequent representations because unintentional phase shifts are often introduced during communication.

The frequency offset Δf_n is given by:

$$\Delta f_n = \frac{k_n}{2T} \tag{6}$$

where k_n is an integer that determines the frequency offset of the nth pulse. In order to accurately represent the

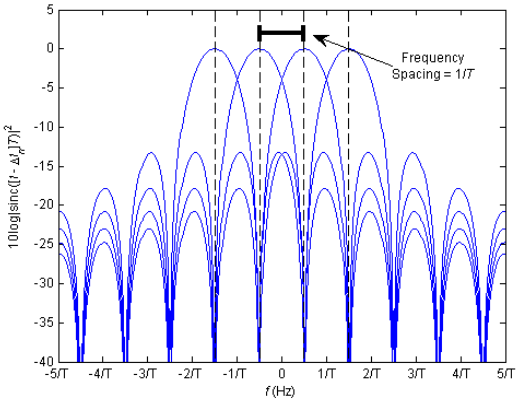

Figure 3: Normalized power spectra for four orthogonally spaced sinc functions. The spacing between any two functions' peaks is $1/T$, so that peaks are centered at the other functions' zero crossings.

Seastar modulation scheme, it is necessary that we adopt $k_n \in \{\pm 1, \pm 3, \ldots, \pm(M-1)\}$. This particular set of k_n ensures that the spectral spacing between each unique frequency is equal to $1/T$ and that the individual pulses are orthogonal, even with phase shift ϵ_n.

The MFSK waveform in the frequency domain is a summation of sinc functions whose peaks occur along the positive frequency axis at $f = f_c + \Delta f_n$, and whose zero crossings occur every $1/T$ from f [5, 6]. As illustrated in Figure (3), the occurrence of a particular sinc function's peak at the zero crossings of the other sinc functions, along with the exact overlapping of the functions' zero crossings, is consistent with the condition of orthogonality.

Now that pure MFSK has been discussed, it is possible to mathematically define the multi-channel MFSK waveform used aboard the Seastar modems. By multi-channel MFSK, we mean to transmit several MFSK pulse trains, or channels, by using frequency-division multiplexing (FDM). Signals that are transmitted using FDM are fed into a modulator that simply sums the signals. Each signal has its own, unique carrier frequency known as a subcarrier frequency. In FDM, the input signals may be modulated using any variety of schemes, including amplitude modulation, phase modulation, frequency modulation, and any of the digital modulation techniques that exist. For Seaweb and Seastar, MFSK has been chosen because it has proven to be a robust and reliable waveform in underwater data transmission [5].

Multi-channel MFSK allows us to transmit I channels of MFSK pulse trains simultaneously. The scheme thus permits data to be transmitted in parallel, allowing for data rates that are higher than a single MFSK pulse train by a factor of I. In the case of Seastar, I = 32 channels (32 pulse trains), and the entire waveform is spread across 5120 Hz of bandwidth [2, 10]. At any particular time during transmission, there are subsequently 32 channels of 4-ary FSK pulse trains, where each subpulse of a particular pulse train has

one of four possible frequencies corresponding to one of the four unique channel symbols.

Combining the mathematical representations of MFSK and FDM, we develop a general and analytical representation for multi-channel MFSK:

$$x(t) = \sum_{i=1}^{I} \sum_{n=1}^{N} x_{n,i}(t - t_n), 0 \leq t \leq T_d \tag{7}$$

where the nth pulse of the ith channel is given by:

$$x_{n,i}(t) = \tag{8}$$
$$A_i \cos(2\pi \left[f_{c,i} + \Delta f_{n,i}\right] t + \epsilon_{n,i}) \text{rect}\Big(\frac{t - 0.5T}{T}\Big)$$

where I is the number of channels, or MFSK pulse trains, N is the number of pulses (channel symbols) transmitted in the time interval $0 \leq t \leq T_d$, t_n is the time instant when the nth pulse begins (seconds), T_d is the duration of the transmitted pulse train (seconds), A_i is the amplitude of the ith channel, $f_{c,i}$ is the subcarrier frequency of the ith channel (hertz), $\Delta f_{n,i}$ is the frequency offset of the nth pulse of the ith channel (hertz), $\epsilon_{n,i}$ is the introduced phase shift of the nth pulse of the ith channel (radians), and T is the pulse duration (seconds).

The frequency offset $\Delta f_{n,i}$ is given by:

$$\Delta f_{n,i} = \frac{k_{n,i}}{2T} \tag{9}$$

where $k_{n,i} \in \{\pm 1, \pm 3, \ldots, \pm(M-1)\}$. The subcarrier frequency may be expressed as:

$$f_{c,i} = f_c + f_i \tag{10}$$

where

$$f_i = \frac{a_i M}{2T} \tag{11}$$

where f_c is the carrier frequency of the entire multi-channel MFSK signal, f_i determines the frequency spacing of the ith channel, and $a_i \in \{\pm 1, \pm 3, \ldots, \pm(I-1)\}$.

In multi-channel MFSK, each subcarrier frequency is orthogonally spaced, which makes it similar to orthogonal frequency-division multiplexing (OFDM). However, though the subcarriers are orthogonal to each other, we restrict ourselves from calling it OFDM, since OFDM does not encode symbols using different frequencies. In multi-channel MFSK, demodulation does not require phase information to be preserved, since symbols are represented in the frequency domain only. With OFDM, symbols can be represented by amplitude, phase, or both, making the modulation scheme vulnerable to phase shifts and amplitude attenuation. Furthermore, the encoding of symbols using phase introduces an additional layer of demodulation and processing that acts as a sink in the very limited power supply of a remote acoustic communication node.

3.2 Bandwidth Scaled Multi-Channel MFSK

Bandwidth scaling is based on the time-frequency scaling property of Fourier analysis, and is currently in use aboard Seastar modems. Implementing multi-channel MFSK using bandwidth scaling simply requires introducing a scaling factor s into Eq.(3). The resulting bandwidth-scaled signal is:

$$x(st) = \sum_{i=1}^{I} \sum_{n=1}^{N} x_{n,i}(st - t_n), 0 \leq t \leq \frac{T_d}{s} \tag{12}$$

where the nth pulse of the ith channel is given by:

$$x_{n,i}(st) = \tag{13}$$
$$A_i \cos(2\pi \left[f_{c,i} + \Delta f_{n,i}\right] st + \epsilon_{n,i}) \text{rect}\Big(\frac{st - 0.5T}{T}\Big)$$

where

$$\text{rect}\Big(\frac{st - 0.5T}{T}\Big) = \begin{cases} 1, & 0 \leq t \leq \frac{T}{s} \\ 0, & \text{otherwise} \end{cases} \tag{14}$$

$$f_i = \frac{a_i M}{2(T/s)} = \frac{s a_i M}{2T} \tag{15}$$

$$\Delta f_{n,i} = \frac{k_{n,i}}{2(T/s)} = \frac{s k_{n,i}}{2T} \tag{16}$$

In implementing multi-channel MFSK using bandwidth scaling, s is chosen to be greater than unity, so that the signal becomes shortened in the time domain and stretched in the frequency domain.

Provided that sufficient bandwidth is available, bandwidth scaling is a useful and practical way to increase the data rate. With $s > 1$, bandwidth scaling is further advantageous in that it becomes less vulnerable to Doppler spread, since the bandwidth of the individual subpulses and the frequency bins are stretched by a factor of s. The values of the Doppler shifts experienced by a particular path consequently become smaller relative to $1/T$. However, for $s > 1$, the signal is more susceptible to ISI due to the shortening of the pulse duration T. In the short-range, high-frequency underwater acoustic communication channel, where a signal is continuously transmitted, it will be shown that a shortened pulse duration T increases the normalized time differences of arrival between the direct path and the next multipath arrivals of a signal, and ultimately increases the time spread of the received signal.

3.3 Frequency Multiplexed Multi-Channel MFSK

In this paper, the term frequency multiplexing as it pertains to multi-channel MFSK refers to the transmission of the original 5 kHz format across additional bands. This modulation technique adds an additional tier of FDM. The frequency-multiplexed multi-channel MFSK signal may be represented in the time domain by:

$$x(t) = \sum_{j=1}^{J} \sum_{i=1}^{I} \sum_{n=1}^{N} x_{n,i,j}(t - t_n), 0 \leq t \leq T_d \tag{17}$$

where the nth pulse of the ith channel in the jth band is given by:

$$x_{n,i,j}(t) = \tag{18}$$
$$A_{i,j}\cos(2\pi\left[f_{c,i,j} + \Delta f_{n,i,j}\right]t + \epsilon_{n,i,j})\text{rect}\Big(\frac{t-0.5T}{T}\Big)$$

where J is the number of bands of multi-channel MFSK, I is the number of channels, or MFSK pulse trains, N is the number of pulses (channel symbols) transmitted in the time interval $0 \leq t \leq T_d$, t_n is the time instant when the nth pulse begins (seconds), T_d is the duration of the transmitted pulse train (seconds), $A_{i,j}$ is the amplitude of the ith channel in the jth band, $f_{c,i,j}$ is the subcarrier frequency of the ith channel in the jth band (hertz), $\Delta f_{n,i,j}$ is the frequency offset of the nth pulse of the ith channel in the jth band (hertz), $\epsilon_{n,i,j}$ is the introduced phase shift of the nth pulse of the ith channel in the jth band (radians), and T is the pulse duration (seconds).

The frequency offset $\Delta f_{n,i,j}$ is given by:

$$\Delta f_{n,i,j} = \frac{k_{n,i,j}}{2T} \tag{19}$$

where $k_{n,i,j} \in \{\pm 1, \pm 3, \ldots, \pm(M-1)\}$. The subcarrier frequency may be expressed as:

$$f_{c,i,j} = f_c + f_{i,j} \tag{20}$$

where

$$f_{i,j} = \frac{a_i M}{2T} + \frac{b_j I M}{2T} \tag{21}$$

where f_c is the carrier frequency of the entire frequency-multiplexed multi-channel MFSK signal, $f_{i,j}$ determines the frequency spacing of the ith channel in the jth band, $a_i \in \{\pm 1, \pm 3, \ldots, \pm(I-1)\}$, and $b_j \in \{\pm 1, \pm 3, \ldots, \pm(J-1)\}$.

Frequency multiplexing allows for higher data rates to be achieved without shortening the pulse duration T. Maintaining a longer pulse duration protects against ISI in the short-range, high-frequency underwater communication channel, and makes the signal more immune to time spread. However, a significant drawback lies in the fact that there is less tolerance for Doppler spread compared to a bandwidth-scaled multi-channel MFSK signal, since the values of the Doppler shifts experienced by a particular path consequently become larger relative to $1/T$.

4 Demodulation

Demodulation is accomplished by examining the frequency content of the multi-channel MFSK signal with the use of the discrete Fourier transform (DFT), computed by the fast Fourier transform (FFT) algorithm, over each pulse duration T. At the receiver, a band-pass filter can be applied across the known operating band of the signal, so that only frequencies at which we expect information are processed. The received signal is then basebanded through heterodyning, and the multi-channel MFSK spectrum is divided into frequency bins that are $1/T$ Hz wide. With an appropriately sized FFT, each bin potentially contains one tonal. If there are 32 channels, or pulse trains, of 4-ary FSK being transmitted, as in the case of Seastar, then 32 of a possible 128 bins would contain energy from a subpulse. The 128 bins are subsequently divided into 32 groups of four, where each of the four bins corresponds to one of the unique channel symbols determined by the M = 4 alphabet. Comparative decision logic is then applied such that the bin containing the greatest amount of energy determines what channel symbol is being received. This approach is implemented in the simulations, but for a single channel of 4-FSK instead of the entire multi-channel MFSK signal.

For the demodulation of the frequency-multiplexed implementation of multi-channel MFSK, a band-pass filter can be applied to isolate the J bands of multi-channel MFSK, and the same FFT demodulation process repeated for each of these bands.

A useful metric in analyzing the performance characteristics of a particular digital modulation scheme is the encoded symbol error rate (SER). The encoded SER is determined by dividing the number of encoded symbol errors in the received signal by the total number of encoded symbols transmitted over the duration of the signal. Encoded symbol errors can result during the demodulation of a signal that is distorted by noise or interference. The encoded SER is used to measure modulation scheme performance in the simulations.

5 Simulations

In order to characterize the performance of bandwidth scaling and frequency multiplexing in various source-receiver geometries, we simulated the modulation, transmission, reception and demodulation of a signal through a channel with multipath propagation. To illustrate these characteristics, several simplifications and assumptions were made in addition to the channel parameters discussed previously. The ultimate aim of these assumptions was to create a frequency-independent channel model and examine what happens to performance in the narrowband as a result of the effects of multipath propagation, source-receiver geometry, and pulse duration.

The simulated signal consisted of only one pulse train of 4-ary FSK centered at 45 kHz, rather than the entire bandwidth-scaled or frequency-multiplexed multi-channel MFSK signal. Faithfully representing a broadband signal such as multi-channel MFSK would involve taking into account frequency-dependent effects on transmission loss. Due to the wideband distortion introduced by the ocean, these effects vary by tens of decibels from one end of the signal's bandwidth to the other, and would thus present a significant degree of complexity to the model [6]. Furthermore, the effects of the fading channel, source-receiver geometry, and pulse duration on modulation scheme performance can still be illustrated with a single pulse train of 4-ary FSK.

The largest bandwidth a single pulse train of 4-ary FSK would occupy in the Seastar network is 640 Hz, associated with a pulse duration of 6.25 ms. Thus, by restricting our simulations to a narrowband pulse train of 4-ary FSK, we can assume transmission loss is flat across the band of the signal [6]. We further assume that the source and receiver are stationary, allowing us to avoid Doppler spreading of the signal. No additional phase shifts are introduced beyond those introduced by the rays' interactions with the pressure release and rigid bottom boundaries, and the frequency response of the transmitter and receiver are assumed to be flat. Finally, the model was noise-free, ensuring that any errors encountered were caused by multipath interference.

5.1 Results

In this section we consider four pulse durations: 6.25 ms and 12.5 ms, both associated with bandwidth-scaled multi-channel MFSK; and 25 ms and 50 ms, both associated with frequency-multiplexed multi-channel MFSK. Channel simulations were run for each of these pulse durations for source-receiver depths of 5 m, 50 m, 100 m, 150 m and 200 m, over ranges between 50 and 500 m. For all pulse durations, a small number of errors were observed only in the case where the source-receiver depth was 5 m, and only between ranges of 50 and 60 m. These results are shown in Figure (4). For this particular shallow source-receiver geometry and noise-free environment, ISI due to multipath propagation appears to be a factor at short ranges. Errors were not observed for the other four source-receiver depths, and no errors were observed in any of the depth configurations beyond a range of 60 m.

To evaluate the potential ISI for each pulse duration and geometry, Eq.(2) was plotted using arrival time data produced by Bellhop. Figures (5) through (8) show Δt_N for each pulse duration. Plotted with Δt_N on each of these figures

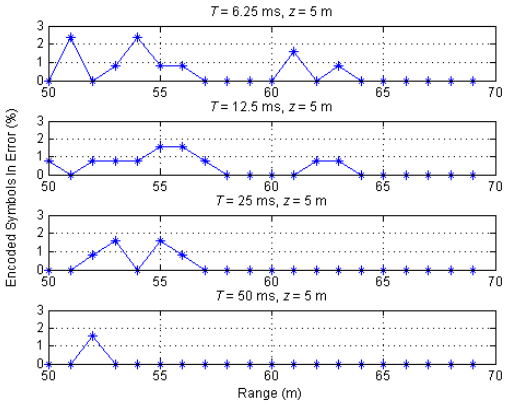

Figure 4: The percentage of encoded symbols received in error are shown for all four pulse durations at a source-receiver depth of z = 5 m and for ranges between 50 and 70 m.

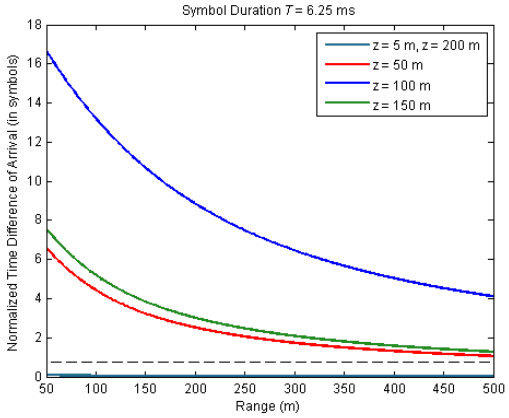

Figure 5: Normalized time difference of arrival between the direct path and the next multipath arrivals for a signal with a pulse duration of 6.25 ms.

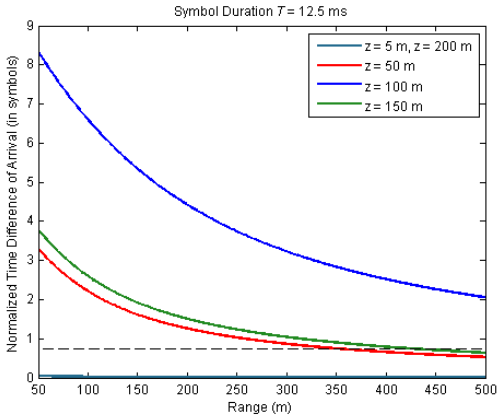

Figure 6: Normalized time difference of arrival between the direct path and the next multipath arrivals for a signal with a pulse duration of 12.5 ms.

is a threshold meant to represent an arbitrary ISI tolerance for a demodulator, and is for illustrative purposes only. The threshold is set for 0.75 symbols, but in reality, a true threshold value would be dependent on the characteristics of the demodulator.

From Figures (5) through (8), we see that for all pulse durations, the normalized time difference of arrival Δt_N is highest at 50 m and lowest at 500 m. Furthermore, the pulse duration is inversely related to Δt_N: shortening the pulse duration will increase Δt_N, and vice versa. We may subsequently conclude that ISI is more likely to occur at shorter ranges than at longer ranges, and for shorter pulse durations than for longer pulse durations. This theoretical evaluation is consistent with the simulation results presented in Figure (4).

According to Figures (5) through (8) and the small values for Δt_N across all ranges for $z = 5$ m and $z = 200$ m,

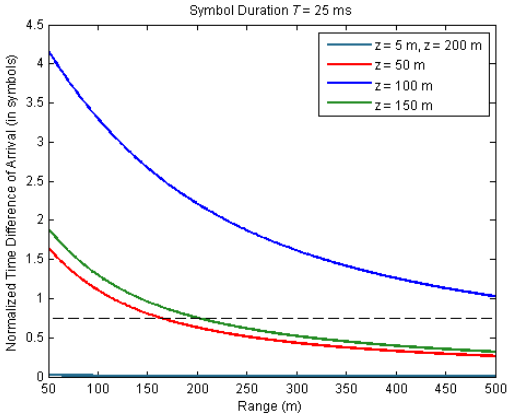

Figure 7: Normalized time difference of arrival between the direct path and the next multipath arrivals for a signal with a pulse duration of 25 ms.

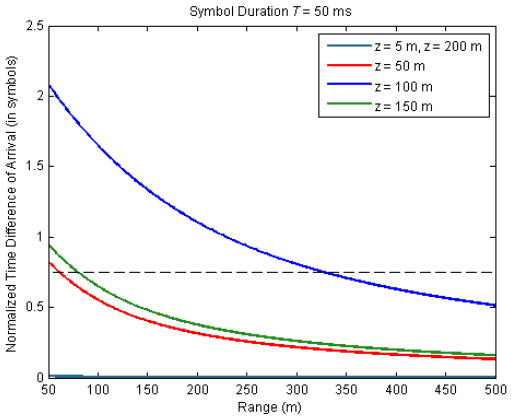

Figure 8: Normalized time difference of arrival between the direct path and the next multipath arrivals for a signal with a pulse duration of 50 ms.

we should not expect ISI to occur, since, for these source-receiver depths, the next multipath signal is nearly synchronized with the direct path signal. However, this expectation directly contradicts the results presented in Figure (4), where errors occurred only at a source-receiver depth of 5 m. Upon closer examination of these signals' characteristics, we find that the amplitude of the next multipath arrival is almost as strong as the direct path signal. Figure (9) shows how the difference in sound pressure level (SPL) between the direct path signal and the next multipath signal is extremely small for z = 5 m and z = 200 m, and much larger for the other source-receiver depths. Thus, despite Δt_N having the smallest values for z = 5 m and z = 200 m, the SPL of the next multipath arrival for these source-receiver depths is also the greatest, and is significant enough to cause ISI for $z = 5$ m.

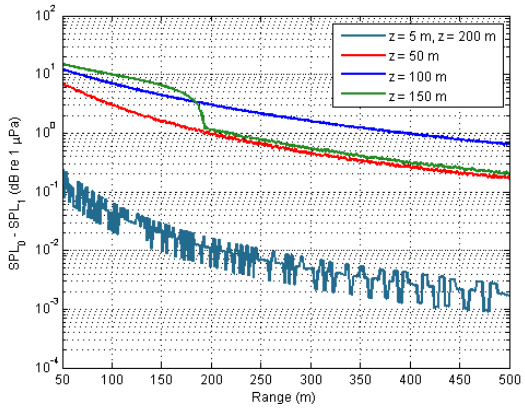

Figure 9: Difference in SPL between the direct path signal and the next multipath arrival.

6 Conclusions

6.1 Findings

The simulations reported in this paper give insight into the relative performance of candidate implementations of multi-channel MFSK. While these results are too preliminary to be used for final design decisions, some general trends are evident that should inform the design and implementation of multi-channel MFSK.

Simulations in a noise-free environment yielded few errors for all pulse durations and geometries. However, lengthening the pulse duration decreases the time difference of arrival between the direct path and the next multipath arrivals and reduces the potential for ISI. Furthermore, because the time difference of arrival decreases as range increases, the potential for ISI also decreases with greater distance between source and receiver.

The demonstrated relationship between pulse duration and time difference of arrival gives support to the frequency multiplexing implementation of multi-channel MFSK over the bandwidth scaling implementation. Consider a frequency-multiplexed implementation with four bands of multi-channel MFSK having a pulse duration of 50 ms. This implementation would have the same data rate as a bandwidth-scaled multi-channel MFSK signal with a pulse duration of 12.5 ms. The frequency multiplexing implementation is therefore the preferable implementation, as it offers the same improved data rate of a bandwidth-scaled signal, but with the added benefit of having a longer pulse duration, thus making it more immune to multipath spread and less susceptible to ISI.

An additional factor in determining which implementation is preferable is the energy per transmitted tone. For instance, in a bandwidth scaling implementation where T = 6.25 ms and the bandwidth is 20 kHz, there is more source energy imparted to the tone in frequency, but for a shorter

period of time. In a frequency multiplexing implementation where $J = 4$ bands and $T = 25$ ms, there is less source energy imparted to the tone in frequency, but for a longer period of time. As the term "scaling" implies, the trade-off in frequency and time is scaleable, and the total energy per transmitted tone remains constant. Thus, in terms of energy per transmitted tone, bandwidth scaling offers no advantages over frequency multiplexing.

6.2 Recommendations

Based on the simulation results, we recommend that steps be taken to implement the frequency-multiplexed version of multi-channel MFSK. While this implementation will require more processing during demodulation than the bandwidth-scaled multi-channel MFSK signal, the penalty paid is small compared to contending with the effects of ISI.

Evaluation of the candidate implementations of multi-channel MFSK would be improved through modeling the wideband multi-channel versions of the signals, rather than just a single pulse train of MFSK. While the single pulse train is useful for illustrative purposes and can give us insight as to what may be expected to happen to the entire multi-channel MFSK signal, an accurate characterization of the channel's effects on the signal cannot be obtained until the full signal is propagated through a more realistic channel model. Such a model would ideally be frequency-dependent, phase-coherent, and representative of the statistical characteristics of the channel boundaries at the surface and bottom.

The design of the demodulator may also be improved by implementing spectral equalization to help offset the frequency-dependent effects of the channel. One way to implement such an equalizer would be to transmit a known wideband signal, analyze its received frequency spectrum to determine the effects of the channel on the signal, and adjust the amplitude weights of the FFT demodulator accordingly. Such a signal—a probe signal—could be transmitted before initiating actual communications, and could be used to calibrate short-range, high-frequency nodes and modems.

In addition to more accurately modeling the wideband implementations of multi-channel MFSK, the effects of including forward error correction (FEC) coding and interleaving to protect against ISI would be extremely useful, as these techniques are currently in use aboard commercial modems used by the US Navy [2]. Simulations using such coding would be more representative of what could be expected in actual testing and experimentation.

Beyond modeling, the various candidate implementations of multi-channel MFSK should be tested first in a laboratory setting, and eventually at sea. Such testing yields important data about what is actually occurring to the signal as it propagates through the underwater acoustic communication channel.

References

[1] J.A. Rice, "Seaweb Underwater Networks," in *Proc. Acoust. 2005, Australian Acoust. Soc. Annu. Conf.*, Busselton, Australia, 2006.

[2] J.A. Rice and D. Green, "Advances in Acoustic Communications and Undersea Networks," in *Proc. MAST 2008 Conf.*, Cadiz, Spain, 2008.

[3] L.J. Ziomek, *Fundamentals of Acoustic Field Theory and Space-Time Signal Processing*. Boca Raton, FL: CRC Press, 1995.

[4] J.T. Hansen, "Link Budget Analysis for Undersea Acoustic Signaling," M.S. thesis, Dept. of Eng. Acoust., Naval Postgraduate School, Monterey, CA, 2002.

[5] B. Kerstens, "A Study of the Seastar Underwater Acoustic Local Area Network Concept," M.S. thesis, Dept. of Eng. Acoust., Naval Postgraduate School, Monterey, CA, 2007.

[6] W.F. Jenkins II, "Time/Frequency Relationships for an FFT-Based Acoustic Modem," M.S. thesis, Dept. of Eng. Acoust., Naval Postgraduate School, Monterey, CA, 2010.

[7] A.L. Maggi and A.J. Duncan. (Accessed Feb. 2010). AcTUP v2.2l^{α} Acoustic Toolbox User-interface & Post-processor: Installation & User Guide. Curtin University of Technology, Centre for Marine Science & Technology. Perth, Australia. [Online]. Available: http://cmst.curtin.edu.au/local/docs/products/actup_v2_2l_installation_user_guide.pdf

[8] L.E. Kinsler, A.R. Frey, A.B. Coppens and J.V. Sanders, *Fundamentals of Acoustics*, 4th ed. New York: John Wiley & Sons, 2000.

[9] J.G. Proakis, *Digital Communications*, 4th ed. New York: McGra-Hill, 2001.

[10] D. Green. (Mar. 2009). Design Specifications, Seaweb Telesonar Header Packet. Teledyne Benthos. North Falmouth, MA. [Print].

[11] H.P.E. Stern, S.A. Hahmoud and L.E. Stern, *Communication Systems Analysis and Design*. Upper Saddle River, NJ: Pearson Education, 2004.

[12] J.G. Proakis and M. Salehi, *Communication Systems Engineering*, 2nd ed. Upper Saddle River, NJ: Pearson Prentice Hall, 2002.

[13] W. Stallings, *Data and Computer Communications*, 8th ed. Upper Saddle River, NJ: Pearson Education, 2007.